2310 *Inorg. Chem.* **2010**, *49*, 2310–2315
DOI: 10.1021/ic902169s

Inorganic Chemistry
Article

Temperature Switch of LMCT Role: From Quenching to Sensitization of Europium Emission in a $Zn^{II}-Eu^{III}$ Binuclear Complex

Traian D. Pasatoiu,[†] Augustin M. Madalan,[†] Michael U. Kumke,[‡] Carmen Tiseanu,[*,§] and Marius Andruh[*,†]

[†]*University of Bucharest, Faculty of Chemistry, Inorganic Chemistry Laboratory, Str. Dumbrava Rosie nr. 23, 020464-Bucharest, Romania,* [‡]*Institute of Chemistry, Physical Chemistry, University of Potsdam, Karl-Liebknecht-Str. 24-25, 14476 Potsdam-Golm, Germany, and* [§]*National Institute for Laser, Plasma and Radiation Physics, Laboratory of Solid-State Quantum Electronics, P.O. Box MG-36, Magurele, 077125, Romania*

Received November 3, 2009

The synthesis, structural investigation, and photophysical properties of a new heterobinuclear complex, $[Zn(H_2O)(valpn)Eu(NO_3)_3]$, are reported [$H_2$valpn = 1,3-propanediylbis(2-iminomethylene-6-metoxy-phenol)]. In the absence of the antenna-type sensitization of europium emission at room temperature, the strongest metal-centered emission was obtained following excitation into the $^7F_0-{}^5D_2$ transition at 535 nm. In contrast, at 80 K, the strongest emission of europium was obtained by exciting into the maximum of a high-intensity, low-lying ligand-to-metal charge-transfer band (LMCT) located at ~425 nm. The overall temperature-induced changes of the photophysical properties of europium were assigned to the relative location of the LMCT and $^3\pi\pi^*$ ligand states to the europium excited levels. The results may explain the lack of the antenna effects reported for some of the europium complexes with this type of ligand.

Introduction

The unique photoluminescent properties of lanthanide (Ln) compounds make them appropriate for a wealth of applications, such as fluorescent lamps, displays, electroluminescent devices, analytical probes, as well as bioprobes for immunoassays or imaging live cells.[1] The applications of their luminescent properties are a consequence of the narrow emission bands, with negligible environmental influences, a large Stokes shift, and relatively long photoluminescence (PL) lifetimes.[2] The disadvantage presented by the very small molar absorption coefficient of f−f transitions[3] is eluded by coordinating organic ligands with a large molar absorption coefficient, resulting in sensitized emission via a so-called antenna effect.[4]

The interest in 3d−4f heterometallic complexes arises from their various properties and applications (chemical sensors, luminescence, catalytic, and magnetic materials).[1,5] A family of ligands widely used in designing such complexes is that of end-off bicompartmental Schiff bases derived from *o*-vanillin and diamines. The two differentiated coordination sites can accommodate, selectively, a 3d and a trivalent 4f ion.[6] The salen-type complexes of zinc (Zn^{2+}) were proved to be efficient sensitizers for the vis as well as NIR emitting trivalent 4f ions.[7] For the case of europium (Eu), the literature is strongly

*To whom correspondence should be addressed. E-mail: tiseanuc@yahoo.com (C.T.), marius.andruh@dnt.ro (M.A.).

(1) See, for example: (a) Eliseeva S. V.; Bünzli, J.-C. G. *Chem. Soc. Rev.*, **2010**, DOI: 10.1039/b905604c.(b) Parker, D. *Coord. Chem. Rev.* **2000**, *205*, 109. (c) De Silva, A. P.; Fox, D. B.; Huxley, A. J. M.; Moody, T. S. *Coord. Chem. Rev.* **2000**, *205*, 41. (d) de Bettencourt-Dias, A. *Dalton Trans.* **2007**, 2229. (e) Hemmila, I.; Laitala, V. *J. Fluoresc.* **2005**, *15*, 529. (f) Bünzli, J.-C. G. *Chem. Lett.* **2009**, *38*, 104.

(2) Bünzli, J.-C. G. In *Lanthanide Probes in Life, Chemical and Earth Sciences. Theory and Practice*; Bünzli, J.-C. G., Choppin, G. R., Eds.; Elsevier Science Publishers B. V.: Amsterdam, 1989.

(3) Carnall, W. T. The Absorption and Fluorescence Spectra of Rare Earth Ions in Solution. In *Handbook on the Physics and Chemistry of Rare Earths*; Gschneidner, K. A., Jr., Eyring, L., Eds.; North Holland Publishing, Co.: Amsterdam, The Netherlands, 1979; Vol. *3*, Chapter 24, pp 172−208.

(4) Weissman, S. I. *J. Chem. Phys.* **1942**, *10*, 214.

(5) See, for example: (a) Andruh, M; Costes, J.-P.; Diaz, C.; Gao, S. *Inorg. Chem.* **2009**, *48*, 3342. (b) Sessoli, R.; Powell, A. K. *Coord. Chem. Rev.* **2009**, *253*, 2328.

(6) Costes, J.-P.; Dahan, F.; Dupuis, A.; Laurent, J.-P. *Inorg. Chem.* **1996**, *35*, 2401.

(7) See, for example: (a) Wong, W.-K.; Liang, H.; Wong, W.-Y.; Cai, Z.-W.; Li, K.-F.; Cheah, K.-W. *New J. Chem.* **2002**, *26*, 275. (b) Wong, W.-K.; Yang, X.; Jones, R. A.; Rivers, J. H.; Lynch, V.; Lo, W.-K; Xiao, D.; Oye, M. M.; Holmes, A. L. *J. Am. Chem. Soc.* **2005**, *127*, 7686. (c) Yang, X.-P.; Jones, R. A.; Wu, Q.-Y.; Oye, M. M.; Lo, W.-K.; Wong, W.-K.; Holmes, A. L. *Polyhedron* **2006**, *25*, 271. (d) Wong, W.-K.; Yang, X.-P.; Jones, R. A.; Rivers, J. H.; Lynch, V.; Lo, W.-K.; Xiao, D.; Oye, M. M.; Holmes, A. L. *Inorg. Chem.* **2006**, *45*, 4340. (e) Lu, X.; Bi, W.; Chai, W.; Song, J.; Meng, J.; Wong, W.-Y.; Wong, W.-K.; Jones, R. A. *New J. Chem.* **2008**, *32*, 127. (f) Lo, W.-K.; Wong, W.-K.; Guo, J.; Wong, W.-Y.; Li, K.-F.; Cheah, K.-W. *Inorg. Chim. Acta* **2004**, *357*, 4510. (g) Lo, W.-K.; Wong, W.-K.; Wong, W.-Y.; Guo, J.; Yeung, K.-T.; Cheng, Y.-K.; Yang, X.; Jones, R. A. *Inorg. Chem.* **2006**, *45*, 9315.

 Published on Web 02/02/2010

supportive for the role of the Schiff base ligand in shaping the emission processes of the lanthanide's ion.[8] No antenna effects were observed with most of the phenoxo-bridged Zn−Eu oligonuclear complexes based on compartmental Schiff-base ligands derived from *o*-vanillin, except the binuclear complex obtained from the N,N′-bis(5-bromo-3-methoxysalicylidene)phenylene-1,2-diamine Schiff base.[7c,8e] Also noticeable is that the absence of the antenna-type sensitization was reported with the mononuclear complexes of europium with this type of ligand as well.[9a,b]

Irrespective of the mononuclear or binuclear type of the europium complex, in the absence of the antenna-type sensitization, no further PL investigation based on the direct excitation into the f−f absorption levels of europium was performed. To get in-depth insights into the photophysics responsible for the lack of the antenna effects, here we analyze the steady-state and time-resolved emission and excitation spectra as well as the excited state dynamics of a new europium complex, $[Zn(H_2O)(valpn)Eu(NO_3)_3]$ [H_2valpn = 1,3-propanediylbis(2-iminomethylene-6-metoxy-phenol]. The strong changes of the photophysical properties of the europium complex with temperature were assigned to the relative location of the triplet state of the ligand and ligand-to-metal charge-transfer (LMCT) band to the metal emissive levels.

Experimental Section

Synthesis and X-Ray Structure Determination. The chemicals used, *o*-vanillin, 1,3-diaminopropane, $Zn(NO_3)\cdot 6H_2O$, $Eu(NO_3)_3\cdot 6H_2O$, $Gd(NO_3)_3\cdot 6H_2O$, and $La(NO_3)_3\cdot 6H_2O$ as well as all the solvents (THF, acetonitrile) were of reagent grade and were purchased from commercial sources.

The mononuclear precursor, $[Zn(valpn)(H_2O)]$, was prepared as follows: To 50 mL of a THF solution containing 20 mmol of *o*-vanillin, 10 mmol of 1,3-diaminopropane and then 20 mmol of triethylamine were added dropwise while continuously stirring. After 30 min, an aqueous solution (50 mL) containing 10 mmol of $Zn(NO_3)_2\cdot 6H_2O$ was added, and the resulting mixture was stirred for an hour, while pouring in 200 mL of H_2O, in order to facilitate the precipitation of the mononuclear complex. The pale yellow solid obtained (yield = 75−80%) was then vacuum filtered and dried. IR spectra and elemental analyses were used to characterize the starting material.

[Zn(valpn)Eu], [Zn(valpn)Gd], and [Zn(valpn)La] Complexes. The synthesis of the binuclear [Zn(valpn)Ln] complexes consists of the addition of 4 mmol of $Ln(NO_3)_3\cdot 6H_2O$ (Ln = Eu, Gd, and La) to a suspension containing 4 mmol of [Zn(valpn)] in 20 mL of acetonitrile, while continuously stirring the reaction mixture for about 30 min. After several days, orange $[Zn(H_2O)(valpn)Eu(NO_3)_3]$, yellow $[Zn(H_2O)(valpn)Gd(NO_3)_3]$, and yellow $[Zn(H_2O)(valpn)La(NO_3)_3]$ crystals of the desired compounds were obtained through the slow vaporization of the solvent. Elemental chemical analyses calcd for $C_{19}H_{22}N_5O_{14}ZnEu$, **1**: C 29.96; H 2.91; N 9.19%. Found: C 30.1; H 2.8; N 9.3%. Calcd for $C_{19}H_{22}N_5O_{14}ZnGd$, **2**: C 29.75; H 2.89; N 9.13%. Found: C 29.6; H 3.0; N 9.4%. Calcd for $C_{19}H_{22}LaN_5O_{14}Zn$, **3**: C 30.48; H 2.96; N 9.35. Found: C 30.2; H 2,9; N 8.9%.

(8) See, for example: (a) Wang, H.; Zhang, D.; Ni, Z.-H.; Tian, X.-L. L.; Jiang, J. *Inorg. Chem.* **2009**, *48*, 5946. (b) Gao, T.; Yan, P.-F.; Li, G.-M.; Hou, G.-F.; Gao, J.-S. *Inorg. Chim. Acta* **2008**, *361*, 2051. (c) Burrow, C. E.; Burchell, T. J.; Lin, P.-H.; Habib, F.; Wernsdorfer, W.; Clérac, R.; Murugesu, M. *Inorg. Chem.* **2009**, *48*, 8051. (d) Zhao, S.; Lu, X.; Hou, A.; Wong, W.-Y.; Wong, W.-K.; Yang, X.; Jones, R. A. *Dalton Trans.* **2009**, 9595. (e) Yang, X.; Hahn, B. P.; Jones, R. A.; Stevenson, K. J.; Swinnea, J. S.; Wu, Q. *Chem. Commun.* **2006**, 3827.

(9) (a) Gao, T.; Yan, P.-F.; Li, G.-M.; Hou, G.-F.; Gao, J.-S. *Inorg. Chim. Acta* **2008**, *361*, 2051. (b) Dou, W.; Yao, J.-N.; Liu, W.-S.; Wang, Y.-W.; Zheng, J.-R.; Wang, D.-Q. *Inorg. Chem. Commun.* **2007**, *10*, 105.

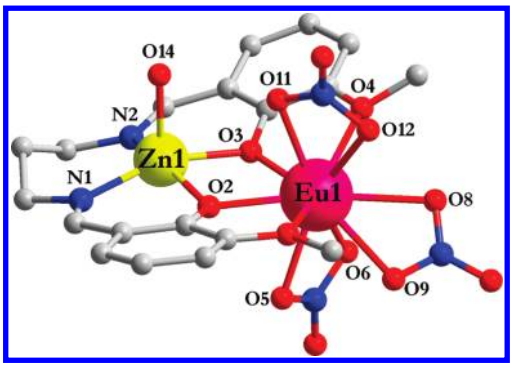

Figure 1. View of the molecular structure for $[Zn(H_2O)(valpn)Eu(NO_3)_3]$.

The obtained crystals were submitted to X-ray diffraction. Atomic scattering factors were taken from the international tables for X-ray crystallography. Hydrogen atoms were included but not refined. Drawings of the molecule were performed with the program Diamond 3. Crystallographic data for the structures reported here have been deposited at the Cambridge Crystallographic Data Centre: CCDC reference numbers 753155, 753156, and 762125.

Optical Characterization. UV−vis−NIR spectra were recorded on a JASCO V-670 spectrophotometer using crushed crystals of the compounds. X-ray data were collected at 293 K on a STOE IPDS II diffractometer using graphite-monochromated Mo Kα radiation sources (λ = 0.71073 Å).

The photoluminescence (PL) measurements were carried out using a Fluoromax 4 spectrofluorometer (Horiba) operated in both the fluorescence and the phosphorescence mode, using fine crystalline powder obtained by crushing the crystals of $[Zn(valpn)Ln(NO_3)_3(H_2O)]$. The repetition rate of the xenon flash lamp was 25 Hz. The integration window varied between 300 ms and 1 s. The delay after flash varied between 0.05 and 10 ms, and 25 up to 100 flashes were accumulated per data point. The slits were varied from 0.1 to 10 nm in excitation as well as emission. PL decays were measured by using the "decay by delay" feature of the phosphorescence mode. Emission and excitation spectra were corrected against spectral response of the detectors. Time resolved emission spectra (TRES) were recorded using a wavelength tunable Nd:YAG-laser/OPO system (Spectra Physics/GWU) operated at 20 Hz as an excitation light source and an intensified CCD camera (Andor Technology) coupled to a spectrograph (MS257 Model 77700A, Oriel Instruments) as a detection system. The TRES were collected using the boxcar technique. Samples were excited in the spectral range of 330−535 nm. The initial gate delay (delay after laser pulse) was set to 500 ns, and the gate width was adjusted to 50 μs. The PL was detected in the spectral range of 400 nm < λ_{em} < 750 nm with a spectral resolution of 0.08 nm. Lamp or laser excited photoluminescence measurements were performed at both room (295 K) and liquid nitrogen temperatures (80 K). For the low-temperature measurements, the solid state samples of Eu or Gd complexes were mounted on a coldfinger attached to a liquid nitrogen Dewar.

Results and Discussion

Crystal Structures. The new heterodinuclear complexes, $[Zn(H_2O)(valpn)Eu(NO_3)_3]$ (**1**), $[Zn(H_2O)(valpn)Gd(NO_3)_3]$ (**2**), and $[Zn(H_2O)(valpn)La(NO_3)_3]$ (**3**), were synthesized in acetonitrile, using stoichiometric amounts of $[Zn(valpn)(H_2O)]$ and $Ln(NO_3)_3\cdot 6H_2O$. The X-ray diffraction showed that the three complexes are isomorphous and crystallize in the $P2_1/c$ monoclinic space group. Therefore, only the molecular structure of **1** is described.

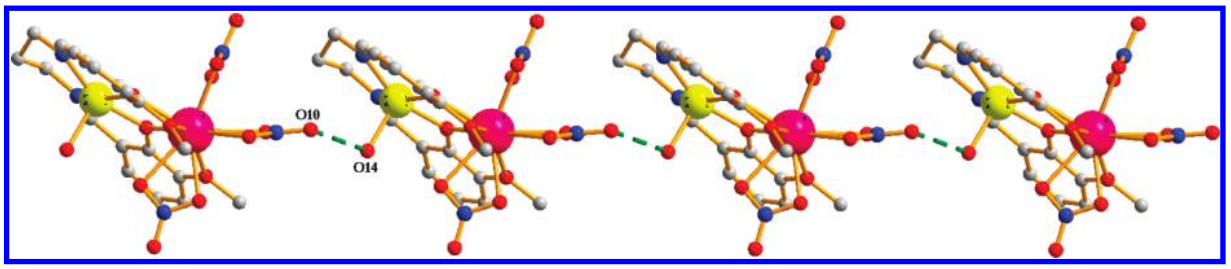

Figure 2. Packing diagram for compound **1** showing the formation of the supramolecular chains.

Table 1. Crystal Data and Refinement for Compounds **1**−**3**

compound	**1**	**2**	**3**
chemical formula	$C_{19}H_{22}N_5O_{14}ZnEu$	$C_{19}H_{22}N_5O_{14}ZnGd$	$C_{19}H_{22}LaN_5O_{14}Zn$
M (g mol^{-1})	761.76	767.05	748.68
temperature, (K)	293(2)	293(2)	293(2)
wavelength, (Å)	0.71073	0.71073	0.71073
cryst syst	monoclinic	monoclinic	monoclinic
space group	*P21/c*	*P21/c*	*P21/c*
a (Å)	8.9419(4)	8.9343(3)	9.0232(6)
b (Å)	29.2149(13)	29.2116(13)	29.027(3)
c (Å)	10.1778(4)	10.1603(3)	10.2900(6)
α (deg)	90.00	90.00	90
β (deg)	103.496(3)	103.538(3)	103.015(5)
γ (deg)	90.00	90.00	90
V (Å^3)	2585.40(19)	2578.01(16)	2625.8(4)
Z	4	4	4
D_c (g cm^{-3})	1.952	1.971	1.889
μ (mm^{-1})	3.411	3.560	2.596
F(000)	1496	1500	1472
goodness-of-fit on F^2	1.075	1.166	1.030
final R_1, wR_2 [$I > 2\sigma(I)$]	0.0544, 0.1151	0.0728, 0.1345	0.0661, 0.1344
R_1, wR_2 (all data)	0.0794, 0.1258	0.0864, 0.1402	0.1180, 0.1523
largest diff. peak and hole (e Å^{-3})	1.537, −1.242	1.181, −1.711	1.303, −1.219

Table 2. Selected Bond Distances for [Zn(H$_2$O)(valpn)Eu(NO$_3$)$_3$] (**1**), [Zn(H$_2$O)(valpn)Gd(NO$_3$)$_3$] (**2**), and [Zn(H$_2$O)(valpn)La(NO$_3$)$_3$] (**3**)

Zn1−N1	2.047(5)	Eu1−O1	2.549(3)
Zn1−N2	2.048(5)	Eu1−O2	2.386(3)
Zn1−O2	2.035(3)	Eu1−O3	2.344(3)
Zn1−O3	2.050(3)	Eu1−O4	2.542(3)
Zn1−O14	2.080(4)	Eu1−O5	2.476(5)
		Eu1−O6	2.488(4)
		Eu1−O8	2.583(4)
		Eu1−O9	2.564(4)
		Eu1−O11	2.514(4)
		Eu1−O12	2.513(4)
Zn1−N1	2.046(6)	Gd1−O1	2.541(4)
Zn1−N2	2.048(6)	Gd1−O2	2.378(4)
Zn1−O2	2.033(4)	Gd1−O3	2.323(4)
Zn1−O3	2.051(4)	Gd1−O4	2.524(4)
Zn1−O14	2.080(5)	Gd1−O5	2.456(6)
		Gd1−O6	2.471(6)
		Gd1−O8	2.591(5)
		Gd1−O9	2.550(5)
		Gd1−O11	2.500(5)
		Gd1−O12	2.501(5)
Zn1−N1	2.050(7)	La1−O1	2.626(4)
Zn1−N2	2.046(6)	La1−O2	2.441(4)
Zn1−O2	2.062(4)	La1−O3	2.481(4)
Zn1−O3	2.047(4)	La1−O4	2.603(4)
Zn1−O14	2.086(5)	La1−O5	2.654(4)
		La1−O6	2.667(4)
		La1−O8	2.623(5)
		La1−O9	2.610(5)
		La1−O11	2.568(6)
		La1−O12	2.568(7)

Its structure consists of neutral [Zn(H$_2$O)(valpn)Eu(NO$_3$)$_3$] entities (Figure 1). The zinc ion displays a square pyramid environment, with a N_2O_2 tetragonal base formed by the donor atoms of the organic ligand and an apical aqua ligand. The europium ion is surrounded by 10 oxygen atoms: two phenolato, two methoxy, and two oxygen atoms from each of the three chelating nitrato ions. The local symmetry at the Ln sites could be approximated with C_2.[10]

At the supramolecular level, the binuclear units interact through hydrogen bonds established between the aqua ligand from one complex (O14) and the oxygen atom (O10) arising from one of the nitrato ligands from another complex, O10···O14 = 2.767 Å, resulting in supramolecular chains running along the crystallographic c axis (Figure 2).

Crystal data collection and refinement parameters as well as selected bond distances for complexes **1**−**3** are given in Tables 1 and 2, respectively.

Europium-Centered Photophysical Properties. Figures 3 and 4 illustrate the relevant photophysical data obtained for the [Zn(H$_2$O)(valpn)Eu(NO$_3$)$_3$] complex at both room-temperature and 80 K. No emission was detected at room temperature following excitation into the ligand maximum absorption, i.e., between 300 and 380 nm (see also Figure S1 in the Supporting Information). The absence of the antenna effect is also confirmed by the PL excitation spectrum of **1** measured at 614 nm. As shown in Figure 3, it displays only the f−f absorption levels of europium starting from the fundamental and thermally populated $^7F_0$ and $^7F_1$. The shape of the excitation spectrum is highly uncommon, as

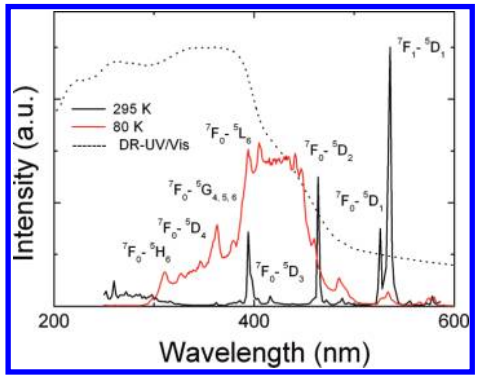

Figure 3. PL excitation spectra of [Zn(H$_2$O)(valpn)Eu(NO$_3$)$_3$] measured at 295 and 80 K at a time delay after the lamp pulse, δt = 50 μs (λ_{em} = 614 nm). Spectra were normalized to the integrated intensity corresponding to the $^7F_0$−$^5D_0$ absorption. With dotted lines is represented the DR/UV−vis spectrum of the same complex.

(10) Vicentini, G.; Zinner, L. B.; Zukerman-Schpector, J.; Zinner, K. *Coord. Chem. Rev.* **2000**, *196*, 353.

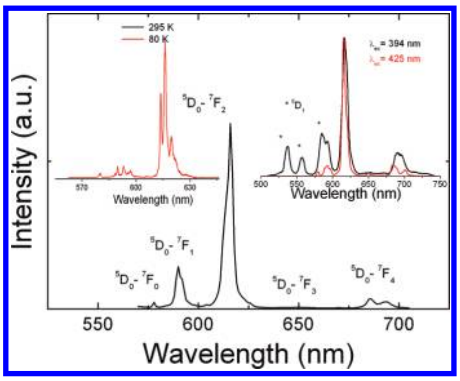

Figure 4. PL emission spectra of $[Zn(H_2O)(valpn)Eu(NO_3)_3]$ measured at 295 K (λ_{ex} = 535 nm, δt = 50 μs). Inset, right: PL emission spectra of $[Zn(H_2O)(valpn)Eu(NO_3)_3]$ measured at 295 K (λ_{ex} = 394 nm) and 80 K (λ_{ex} = 425 nm) at δt = 1.5 μs. Inset, left: High resolution PL emission spectrum of $[Zn(H_2O)(valpn)Eu(NO_3)_3]$ measured at 80 K at δt = 30 μs.

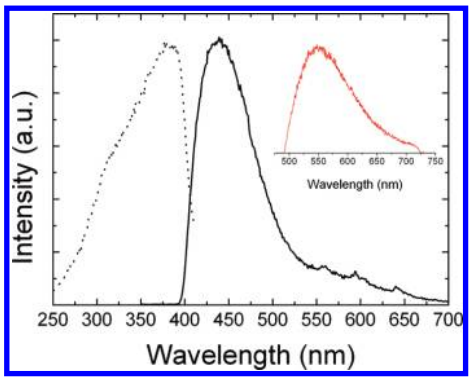

Figure 5. Fluorescence emission (continuous line, λ_{em} = 370 nm) and excitation spectra (dotted line, λ_{ex} = 435 nm) of the Gd complex (**2**) measured at 295 K. The sharp rise at ~400 nm is related to use of a 400 nm cutoff filter. Inset: Phosphorescence spectrum of the Gd complex measured at 80 K as a powder state (λ_{ex} = 380 nm; time delay after the flash lamp, δ = 100 μs).

strong absorption at 525 or 535 nm relative to other f−f absorption levels of europium is rarely observed.[11]

Lowering the temperature at 80 K, the shape of the excitation spectrum has dramatically changed. A broad band that peaked at about ~425 nm, with tails extending from 300 to 600 nm, was observed together with the f−f absorptions of europium (see also Figure S2, Supporting Information). The shape of the short-wavelength region with a broad envelope peaking at about 350 nm resembles the ground state ligand absorption ($^1\pi\pi^*$ transition). This means that, at low temperatures, excitation via the ligand is functional, with efficiency close to that of direct excitation (see also Figure S3a, Supporting Information).

Figure 4 gathers some representative emission spectra of europium excited at various excitation wavelengths (see also Figures S3 and S6, Supporting Information). At room temperature, europium emission was excited by using 394, 464, or 535 nm excitation wavelengths. As expected from the shape of the excitation spectrum, excitation at 535 nm was leading to the strongest $^5D_0$ based emission. Besides the $^5D_0$ related transitions (corresponding to $^5D_0$−$^7F_{0-4}$ transitions at 579, 582, 614, 653, and 698 nm, respectively), $^5D_1$ related emission was also observed in the spectral range of 520−600 nm (see also Figure S4, Supporting Information). At 80 K, the intensity of the europium emission was increased upon excitation into the 425 nm centered band. No $^5D_1$ emission could be detected following excitation into the broad band, pointing to the different population mechanisms of the $^5D_0$ level with the temperature (Figure 4, right).

Several features can be outlined from the analysis of the luminescence spectra measured at both 295 and 80 K. The detection of the low intensity, electric, and magnetic dipole forbidden $^5D_0$−$^7F_0$ transition is in line with the low symmetry environment (C_2) at the europium sites inferred from the X-ray data. Three lines in the range of the $^5D_0$−$^7F_1$ emission were observed at 80 K, giving support for the existence of a single average europium species (Figure 4, left). The shape of the 0−0 transition is single Gaussian with a relatively large fwhm value of 28 ± 0.2 cm^{-1} (295 K). At 80 K, this transition was narrowed only marginally, to 24 ± 0.3 cm^{-1}, and red-shifted by 8 cm^{-1} from 17249 ± 0.3 cm^{-1} to 17241 ± 0.3 cm^{-1}. Another feature of interest is the high intensity of the $^5D_0$−$^7F_2$ transition, relative to the $^5D_0$−$^7F_1$ lines (asymmetry ratio, R = 4.6). The R value was measured from the time-resolved PL spectra at a time delay of 30 μs after the laser pulse to neglect the contribution of the upper excited states to the $^5D_0$ emission (see also Figure S4, Supporting Information). Vibronic sidebands associated with electronic transitions were also identified in the luminescence spectra, but their analysis is out the scope of this paper.

A strong role of the temperature on the europium photophysics was further evidenced with the excited-state dynamics measurements. The PL decay of europium measured at 614 nm is single exponential at both 295 and 80 K, further supporting the presence of a single emissive center (Figure S5, Supporting Information). Lowering the temperature at 80 K, the PL lifetime increased by 150% from 190 ± 8 μs to 480 ± 8 μs. In contrast, the PL decay measured at 535 nm (corresponding to $^5D_1$ emission) remained fairly constant with the temperature at about 4 ± 0.3 μs.

Ligand-Centered Photophysical Properties. To assess the role of the triplet state in shaping the europium emission, we have also prepared the isostructural gadolinium complex, **2**. The lowest-lying excited level of the Gd ion ($^6P_{7/2}$, at 32 150 cm^{-1}) is higher than the singlet and triplet state of the ligand, and therefore the energy cannot be transferred from the ligand to the gadolinium ions. Hence, the Gd complex displays essentially the same fluorescence and phosphorescence features as the free ligand. Figure 5 illustrates the fluorescence and excitation spectra as well as the phosphorescence spectrum measured at 80 K. Following excitation in the spectral range of 300−390 nm, the emission (fluorescence) corresponding to the $^1\pi\pi^*$ of the Gd complex was obtained centered at about 435 nm.

In addition, a tail extending up to 700 nm was observed. The phosphorescence nature of this long wavelength emission was further confirmed by the time-resolved PL measurements at 80 K. The $^3\pi\pi^*$ triplet state displayed an unstructured phosphorescence that peaked at about 550 nm (or ~18 180 cm^{-1}). The triplet energy values for the binuclear complexes with this type of ligand are scarcely reported in the literature,[7f,g] our value being shifted

(11) Roof, I. P; Smith, M. D.; Park, S.; zur Loye, H.-C. *J. Am. Chem. Soc.* **2009**, *131*, 4202.

toward the blue by 35 nm compared to those reported for the Zn−Gd complex with *N*,*N*′-bis(3-methoxy-5-p-tolylsalicylidene)ethylene-1,2-diamine[7f] or by 30 nm for the ethylene bridged Zn−Gd complexes L = *N*,*N*′-bis(3-methoxysalicylidene)phenylene-1,2-diamine) or *N*,*N*′-bis(3-methoxy-5-p-tolylsalicylidene)phenylene-1,2-diamine.[7g] The excitation spectrum of $^1\pi\pi^*$-related emission measured at 435 nm reveals a strong band peaking at 380 nm with a spectral shoulder located at about 310−320 nm.

Quenching Processes of Europium Emission. It is well-known that several conditions should be fulfilled when selecting the best antenna chromophore in terms of efficient intramolecular energy transfer (IET) to the Ln ion:[1a−c] it should (i) have large extinction coefficients, (ii) have an intersystem crossing (ISC) quantum yield near unity or an energy gap between the singlet and triplet states of the ligand of at least 5000 cm^{-1}, (iii) have a triplet state that is close enough in energy to the lanthanide's emitting state to allow for the effective ligand-to-Ln IET, (iv) protect the Ln from the quenching effects of bound solvent molecules, and (v) keep as low as possible the other competing nonradiative relaxation processes with the Ln emission induced by ligand-to-metal charge transfer (LMCT) or back-transfer from the Ln excited state to the triplet state. As concluded from the X-ray structural determination, no water molecules are bound to europium. Further, Eu−Eu distances are 8.320 Å which precludes any significant ion−ion interactions. Finally, the difference ΔE ($^1\pi\pi^* - {}^3\pi\pi^*$) of ∼ 4880 cm^{-1} determined with the Gd complex is close to the optimum value (5000 cm^{-1}) that enables an efficient IET.[12] The balance between the radiative and nonradiative processes occurring in the excited $^5D_0$ state of europium can be easily assessed by using the simple empirical equation of Werts and co-authors.[13] Accordingly, a value of 2.66 ms was found for the calculated radiative lifetime of europium emission in complex **1**, which should be compared with the measured value of only 190 μs. Further, the intrinsic quantum efficiency of the Eu emission following direct excitation at 535 nm was estimated at 8%. The above values are indicative for a europium environment with strong thermally activated nonradiative processes with rate values as high as 4890 s^{-1}. These processes are related to the thermally activated back-transfer from the europium $^5D_0$ excited state to the triplet state and the ligand-to-metal charge transfer (LMCT) band.[14,8d]

The PL data with the Gd complex (**2**) locates the triplet level between the $^5D_1$ and $^5D_0$ states at roughly 950 cm^{-1} higher than the $^5D_0$ level of europium. According to the more general rule of Latva et al., a difference of 2500 $cm^{-1} < \Delta E(^3\pi\pi^* - {}^5D_0) < 3500$ cm^{-1} is required for an optimal ligand-to-europium metal energy transfer process.[15a] The simple phenomenological energy gap rule applied to the europium case should be amended depending on the ligand[1a] as revealed by the few examples listed below. Indeed, large quantum emission yields were obtained with a difference $\Delta E(^3\pi\pi^* - {}^5D_0)$ of only 750 cm^{-1} (for the case of terfluorene complexes of europium)[15b] or even as low as 300 cm^{-1} (for the case of several Schiff-base complexes of europium).[15c] In contrast, an unusually low efficiency of IET from the triplet of dipyrazolyltriazine derivatives to the coordinated Eu was reported for $\Delta E(^3\pi\pi^* - {}^5D_0)$ of 1600 cm^{-1}.[15d] Further, it was reported that, for a series of europium helicates with a similar value of $\Delta E(^3\pi\pi^* - {}^5D_0)$, the overall quantum yields were found to differ by a factor of 4.[15e] Both the singlet and triplet states of the ligand may serve as donor states in transferring the excitation energy to the europium ions.[1,15d] However, since the singlet state is short-lived, IET via the triplet state is considered as the dominant pathway. Besides the ligand type, the position of the triplet state should be considered in conjunction with a number of factors, such as the temperature-dependent overlap integral between the normalized emission spectrum of the donor ($^3\pi\pi^*$) state and the normalized absorption spectrum of the acceptor state.[15f] On the other hand, the presence of a high-intensity LMCT band close to the singlet state is clearly evidenced with the excitation spectrum of $^5D_0$ emission at 80 K. The width of the LMCT band of ca. 6000 cm^{-1} is consistent with typical values of lanthanide CT bands (i.e., between 5000 and 10 000 cm^{-1})[16] allowing for the extension of the excitation window of europium emission up to 500 nm (Figure 3). According to the comprehensive theoretical model developed by Faustino et al.,[14k] the LMCT lies in the "good" spectral region (i.e., between the $^5D_3$ (416 nm) and $^5D_2$ (464 nm) levels). This is expected to induce only a small reduction of the overall quantum yield of europium emission. The excitation energy follows the path LMCT → $^3\pi\pi^*$ → $^5D_0$, as inferred from the absence of the $^5D_1$ emission upon excitation into this band (Scheme 1). Such a conclusion is based on an extensive series of time-resolved PL measurements at both 295 and 80 K by using several excitation wavelengths within the LMCT band: part of the excitation wavelengths corresponded to the superimposed f−f transitions of europium (i.e., 394 and 464 nm corresponding to the $^7F_0-{}^5L_6$ and $^7F_0-{}^5D_2$, respectively), while the rest of them were chosen outside the f−f absorptions (i.e., at 425, 440, and 485 nm). A selection of the time-resolved

(12) Steemers, F. J.; Verboom, W.; Reinhoudt, D. N.; Vandertol, E. B.; Verhoeven, J. W. *J. Am. Chem. Soc.* **1995**, *117*, 9408.
(13) Martinus, H.; Werts, V.; Ronald, Y.; Jukes, T. F.; Verhoeven, J. W. *Phys. Chem. Chem. Phys.* **2002**, *4*, 1542.
(14) See, for example: (a) Blasse, G. *Struct. Bonding* (*Berlin*) **1976**, *26*, 43. (b) Napier, G. D. R.; Neilson, J. D.; Shepherd, T. M. *Chem. Phys. Lett.* **1975**, *31*, 328. (c) Chelebaeva, E.; Larionova, J.; Guari, Y.; Ferreira, R. A. S.; Carlos, L. D.; Almeida Paz, F. A.; Trifonov, A.; Guerin, C. *Inorg. Chem.* **2009**, *48*, 5983. (d) Gawryszewska, P.; Legendziewicz, J. *J. Lumin.* **2007**, *496*, 122. (e) Faustino, W. M.; Malta, O. L.; Teotonio, E. E. S.; Brito, H. F.; Simas, A. M.; de Sa, G. F. *J. Phys. Chem. A* **2006**, *110*, 2510. (f) Puntus, L. N.; Chauvin, A. S.; Varbanov, S.; Bünzli, J. C.-G. *Eur. J. Inorg. Chem.* **2007**, 2315. (g) Shavaleev, N. M.; Eliseeva, S. V.; Scopelliti, R.; Bünzli, J. C.-G. *Chem. Eur. J.* **2009**, DOI: 10.1002/chem.200901996.(h) Puntus, L. N.; Lyssenko, K. A.; Pekareva, I.; Bünzli, J.-C. G. *J. Phys.Chem. B* **2009**, *113*, 9265. (i) Goncalves e Silva, F. R.; Longo, R.; Malta, O. L.; Piguet, C.; Bünzli, J.-C. G. *Phys. Chem. Chem. Phys.* **2000**, *2*, 5400. (j) Berry, M. T.; May, P. S.; Xu, H. *J. Phys. Chem.* **1996**, *100*, 9216. (k) Faustino, W. M.; Malta, O. L.; de Sa, G. F. *J. Chem. Phys.* **2005**, *122*, 054109.
(15) (a) Latva, M.; Takalo, H.; Mukkala, V.-M.; Matachescu, C.; Rodriguez-Ubis, J. C.; Kankare, J. *J. Lumin.* **1997**, 75. (b) Oxley, D. S.; Walters, R. W.; Copenhafer, J. E.; Meyer, T. Y.; Petoud, S.; Edenborn, H. M. *Inorg. Chem.* **2009**, *48*, 6332. (c) Archer, R. D.; Chen, H. Y.; Thompson, L. C. *Inorg. Chem.* **1998**, *37*, 2089. (d) Yang, C.; Fu, L.-M.; Wang, Y.; Zhang, J.-P.; Wong, W.-T.; Ai, X.-C.; Qiao, Y.-F.; Zou, B.-S.; Gui, L.-L. *Angew. Chem., Int. Ed.* **2004**, *43*, 5010;(e) Chauvin, A.-S.; Comby, S.; Baud, M.; De Piano, C.; Duhot, C.; Buunzli, J.-C. G. *Inorg. Chem.* **2009**, *48*, 10687. (f) Dexter, D. L. *J. Chem. Phys.* **1953**, *21*, 836.
(16) Liu, G. K.; Jensen, M. P.; Almond, P. M. *J. Chem. Phys. A* **2006**, *110*, 2081.

Scheme 1. Simplified Diagram of Photophysical Processes in the [Zn(H_2O)(valpn)Eu(NO_3)$_3$] Complex[a]

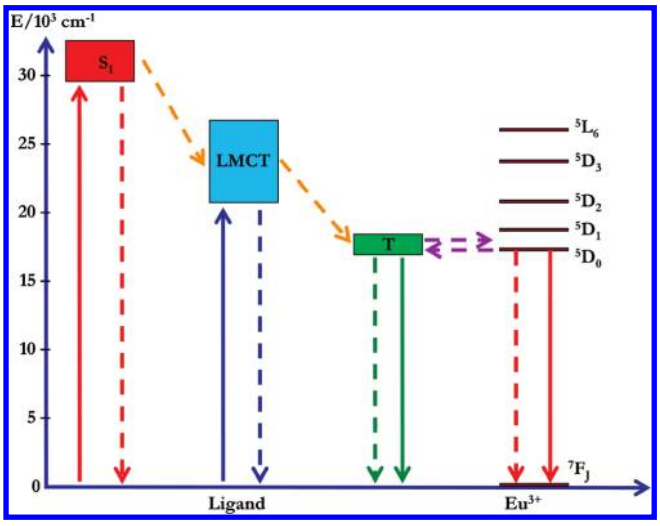

[a] Notations: S1, singlet state; T, triplet state; LMCT, ligand-to-metal charge-transfer state. Dotted and solid lines represent the nonradiative and radiative processes, respectively.

PL spectra is represented in Figure S6 (Supporting Information).

As far as the room-temperature excitation spectrum is concerned (Figure 3), the unusual large absorption intensities of $^7F_{0,1}-{}^5D_1$ transitions relative to those of $^7F_0-{}^5D_2$ (at 464 nm) or $^7F_0-{}^5L_6$ (at 394 nm) may be the result of the spectral superposition between the latter f−f transitions with the broad LMCT state. Due to the efficient thermally activated back-transfer to the triplet state, excitation at 394 or 464 nm leads only partially to the $^5D_0$ emission, and therefore, the intensities of the $^7F_{0,1}-{}^5D_1$ transitions appear as enhanced relative to the rest of the f−f transitions. The comparison between the excitation spectrum of europium emission at room temperature and the peak-deconvoluted one at 80 K is illustrated in Figure S2 (Supporting Information).

The observation at low temperatures of an intense, sensitizing LMCT band is an interesting result. To our knowledge, such intense LMCT bands are seldom detected experimentally,[14f,h] being assigned to the mixing of the intraligand (ILCT) and ligand-to-europium charge transfer (LMCT) states.[14f] To assess if a similar phenomenon occurs with our complexes, we have synthesized a third complex, [Zn(H_2O)(valpn)La(NO_3)$_3$], **3**. According to the X-ray structural determination, complex **3** is isostructural with complexes **1** and **2**. The DR-UV/vis spectra gathered in Figure S1 (Supporting Information) display a common spectral shoulder between 400 and 500 nm whose intensity is clearly enhanced in the spectrum of complex **1**. Overall, the above data support the presence of a LMCT band in the Eu complex at about 425 nm whose high intensity is most probably increased at the expense of the intensity of a closely located intraligand charge transfer band (ILCT).

Conclusion

A new heterodinuclear complex, [Zn(H_2O)(valpn)Eu(NO_3)$_3$], was synthesized and characterized. No ligand sensitization of europium $^5D_0$ based emission was detected at room temperature. In contrast, a complex picture of excitation mechanisms of europium emission was revealed at 80 K as a result of the interplay between an intense, 425 nm centered LMCT band and a $^3\pi\pi$ ligand state close to the $^5D_0$ emissive state of europium ions. Further work will assess the capability of this class of ligands to act as antenna type sensitizers for the lanthanide's emission in the vis and NIR spectral ranges.

Acknowledgment. Finacial support from the CNCSIS (grant IDEI 506/2009) is gratefully acknowledged. C.T. acknowledges A. Gessner from Potsdam University, Germany for performing the low-temperature photoluminescence measurements.

Supporting Information Available: X-ray crystallographic data of complexes **1**−**3** in CIF format, DR-UV/vis spectra of complexes **1**−**3**, steady-state and time-resolved excitation and emission spectra of complex **1** at 80 and 295 K. This material is available free of charge via the Internet at http://pubs.acs.org.